

## **HIGH-ORDER COMPACT FINITE DIFFERENCE SOLUTION OF NAVIER-STOKES EQUATIONS**

Mahmood K. Mawlood, Waqar Asrar\*, ShahNor Basri  
Department of Aerospace Engineering  
and  
Megat M. H. M. Ahmad  
Department of Mechanical and Manufacturing Engineering  
  
Faculty of Engineering  
Universiti Putra Malaysia  
43400 UPM, Serdang, Selangor D. E.  
MALAYSIA

### **ABSTRACT**

*This work involves the application and testing of a Hermitian fourth-order accurate compact finite-difference scheme for solving the two-dimensional, incompressible, Navier-Stokes equations in vorticity-stream function form. The steady, laminar flow in the inlet section of a 2-D channel and the flow in a driven square cavity are studied. The time dependent form of the Navier-Stokes equations are solved by an implicit ADI procedure until the steady state solutions are obtained. Results obtained are found to compare favorably with data published in the literature.*

*Keywords:* High-order compact schemes; channel flow; driven cavity flow.

### **1.0 INTRODUCTION**

High-order compact schemes have attracted much attention in recent years due to their narrow grid stencil and a possible enhanced accuracy over the non-compact schemes [1]. Different approaches for high-order compact spatial discretization have been proposed during the last 25 years.

Hirsh [1] has conducted numerical experiments with a class of fourth-order accurate compact schemes known as Hermitian. The fundamental idea behind this scheme is that the derivatives are treated as unknowns at each point of the computational grid. A system of high-order relations is then needed to approximate the derivatives. To reduce the number of additional equations, Adam [2] has proposed two different techniques to eliminate the second order derivatives in parabolic equations. Adam [2] has also derived additional boundary relations to solve the resulting tridiagonal system of equations.

Lele [3] has presented and analyzed more generalized forms of the Hermitian schemes and introduced the notion of resolution efficiency as a measure of

---

\* The author whom correspondence should be addressed, email: waqar@eng.upm.edu.my

accuracy. Lele [3] has also developed compact schemes for cell-centered meshes. The Hermitian approach has been used by many other workers [4-6].

Rubin and Khosla [7] and Luchini [8] have developed high-order compact schemes from interpolating polynomials. A different approach for obtaining high-order compact schemes has been developed by MacKinnon and Carey [9] and Abarbanel and Kumar [10] independently about the same time. The technique is based on the spatial implementation of the temporal differencing idea of Lax and Wendroff [11]. In this approach the governing equation is utilized to approximate the leading truncation error terms of the standard  $O(h^2)$  central differencing scheme. The schemes developed and used by [12-14] are based on this approach.

It can be noted that all the high-order schemes cited above may be grouped under three general approaches, namely, the Hermitian, the interpolation polynomial and the Lax-Wendroff approaches. The most popular approach seems to be the Hermitian due to its spectral-like characteristics [3] and ease of implementation.

This work is motivated by the desire to develop an algorithm for solving the 2-D Navier-Stokes equations in vorticity-stream function form using a fourth-order Hermitian compact scheme. The problems of laminar incompressible fluid flow in the inlet section of a 2-D channel and the driven cavity flow are considered as testing models. Results are compared with data published in the literature.

## 2.0 THE FOURTH-ORDER COMPACT SCHEME

As mentioned above, the high-order accuracy of the Hermitian scheme is achieved by treating the derivatives as unknowns at the grid points and calculating them from implicit high order relations. A fourth-order approximation to the first derivative,  $F$ , for the function,  $f$ , can be obtained by [1,3]

$$0.25 F_{i-1} + F_i + 0.25 F_{i+1} = 1.5 \left( \frac{f_{i+1} - f_{i-1}}{2h} \right) \quad (1)$$

where  $h$  is the mesh size.

The fourth-order approximation  $S$ , to the second derivative is written as [1,3]

$$0.1 S_{i-1} + S_i + 0.1 S_{i+1} = 1.2 \left( \frac{f_{i+1} - 2f_i + f_{i-1}}{h^2} \right) \quad (2)$$

Boundary conditions for the first and second derivatives must be provided in addition to those of the governing equations. A review of various possible approaches for obtaining boundary relations is presented in [15]. In this work the following high-order implicit relation [15] is used as a boundary relation for the

first derivatives, whereas second derivatives are evaluated by satisfying the governing equations on the boundaries.

$$f_i - f_{i+1} + \frac{h}{2} (F_i + F_{i+1}) + \frac{h^2}{12} (S_i - S_{i+1}) + O(h^5) = 0 \quad (3)$$

### 3.0 METHOD OF SOLUTION

The fourth-order compact scheme is used to solve the two-dimensional, incompressible Navier-Stokes equations in vorticity-stream function ( $\zeta - \psi$ ) form. The unsteady equations for the vorticity and stream function in non-dimensional form are [1,12]

$$\frac{\partial \zeta}{\partial t} + u \frac{\partial \zeta}{\partial x} + v \frac{\partial \zeta}{\partial y} = \frac{1}{Re} \left( \frac{\partial^2 \zeta}{\partial x^2} + \frac{\partial^2 \zeta}{\partial y^2} \right) \quad (4)$$

$$\frac{\partial \psi}{\partial t} - \zeta = \frac{\partial^2 \psi}{\partial x^2} + \frac{\partial^2 \psi}{\partial y^2} \quad (5)$$

Eqs. (4) and (5) are discretized by an ADI procedure [1] to give

$$\begin{aligned} \frac{1}{\Delta t/2} (\zeta_{ij}^{k+1/2} - \zeta_{ij}^k) + u_{ij+}^k FXZ_{ij}^{k+1/2} + v^k FYZ^k \\ = \frac{1}{Re} (SXZ_{ij}^{k+1/2} + SYZ_{ij}^k) \end{aligned} \quad (6a)$$

$$\begin{aligned} \frac{1}{\Delta t/2} (\zeta_{ij}^{k+1} - \zeta_{ij}^{k+1/2}) + u_{ij}^k FXZ_{ij}^{k+1/2} + v^k FYZ_{ij}^{k+1} \\ = \frac{1}{Re} (SXZ_{ij}^{k+1/2} + SYZ_{ij}^{k+1}) \end{aligned} \quad (6b)$$

$$\frac{1}{\Delta t/2} (\psi_{ij}^{k+1/2} - \psi_{ij}^k) - \zeta_{ij}^{k+1} = SX\psi_{ij}^{k+1/2} + SY\psi_{ij}^k \quad (7a)$$

$$\frac{1}{\Delta t/2} (\psi_{ij}^{k+1} - \psi_{ij}^{k+1/2}) - \zeta_{ij}^{k+1} = SX\psi_{ij}^{k+1/2} + SY\psi_{ij}^{k+1} \quad (7b)$$

where  $FXZ$ ,  $FYZ$ ,  $SXZ$ ,  $SYZ$ ,  $SX$  and  $SY$  are the fourth-order approximations to  $\partial \zeta / \partial x$ ,  $\partial \zeta / \partial y$ ,  $\partial^2 \zeta / \partial x^2$ ,  $\partial^2 \zeta / \partial y^2$ ,  $\partial^2 \psi / \partial x^2$  and  $\partial^2 \psi / \partial y^2$  respectively. The superscript  $k$  corresponds to the previously computed or known values,  $k+1/2$  denotes the unknown values at the half-time step and  $k+1$  is the new time level.

Starting with Eqs. (6), at each half-time step of the ADI procedure a block tridiagonal matrix is inverted for  $\zeta$  and its derivatives. Eq. (6a) and the two high-order relations (1) and (2) are solved first for the unknowns  $\zeta_{ij}^{k+1/2}$ ,  $FXZ_{ij}^{k+1/2}$  and  $SXZ_{ij}^{k+1/2}$  in the x-direction (x-sweep). Then, Eq. (6b) with the two high-order relations, are solved for the unknowns  $\zeta_{ij}^{k+1}$ ,  $FYZ_{ij}^{k+1}$  and  $SYZ_{ij}^{k+1}$  in the y-direction (y-sweep). A time-step is considered complete once x-sweeps for all the rows followed by the y-sweeps for all the columns are completed. The stream function values are updated at the new time level  $k+1$ , by solving Eqs. (7a) and (7b) in the same manner.

#### 4.0 RESULTS

The following two problems are solved by the method just described.

**Problem 1.** Laminar flow in the inlet section of 2-D channel:

The flow geometry is shown in Fig. 1. Due to symmetry, only the upper half of the channel is considered. The computational domain starts at a distance  $L_U$  upstream the leading edge of the channel and extends to a distance  $L_D$  downstream the leading edge. Spatz [12] has shown that for low Reynolds number ( $Re \rightarrow 0$ ), the effects of the plates can be felt reasonably ahead of the leading edge, requiring at a minimum that  $L_U = 2H$ .  $L_D$  is long enough for the flow to become fully developed. The boundary conditions are as follows:

At the upstream boundary,

$$u = 1, v = 0, \psi = y, \zeta = 0.$$

At the downstream boundary,

$$u = \frac{3}{2}(1 - y^2), v = 0, \psi = \frac{3}{2}y - \frac{1}{2}y^3, \zeta = 3y.$$

Along the plate, where  $x > 0, y = 1$ ,

$$u = 0, v = 0, \psi = 1.$$

The vorticity,  $\zeta$  along the wall is obtained by writing Eq. (3) for the stream function  $\psi$  on the plate. The remainder of the top boundary, where  $y = 1, x < 0$ ,

$$\psi = 1, v = 0, \zeta = 0.$$

Along the lower boundary, which is a symmetry line,

$$\psi = 0, v = 0, \zeta = 0.$$

The x-component of the velocity,  $u$ , on the top and bottom symmetry lines is calculated as a part of the solution. Solutions are obtained for Reynolds numbers  $Re = 0.5$  and  $Re = 50$  on uniform grids  $65 \times 9$  and  $99 \times 9$ , respectively. The studied Reynolds numbers are the same as those considered by Spatz [12], for comparison. In Figs. 2-4 stream function contours, vorticity contours and x-component of the velocity along the center streamline and the stagnation streamline are compared with the high-order results of Spatz [12]. Figs. 5-7 present the same type of plots for  $Re = 50$ . All these comparisons show that the present results are identical with Spatz's [12] high-order results.

**Problem 2.** The driven cavity flow:

The geometry of this problem consists of a square cavity  $[0,1] \times [0,1]$ , as shown in Fig. 8, filled with an incompressible fluid. At the initial time the upper wall is given a unit velocity and the final steady state solution is sought. The boundary conditions that can be specified are, on the four walls

$$\begin{aligned} \psi &= const = 0, \\ \frac{\partial \psi}{\partial x} &= -v, \quad \frac{\partial \psi}{\partial y} = u, \end{aligned}$$

and

$$\begin{aligned} \frac{\partial^2 \psi}{\partial y^2} &= 0, \quad \frac{\partial^2 \psi}{\partial x^2} = -\zeta, \quad x = 0 \text{ and } x = 1, \\ \frac{\partial^2 \psi}{\partial x^2} &= 0, \quad \frac{\partial^2 \psi}{\partial y^2} = -\zeta, \quad y = 0 \text{ and } y = 1. \end{aligned}$$

The boundary values for vorticity along the four walls are obtained by writing Eq. (3) for the stream function along the walls. The velocity boundary conditions on the four walls are shown in Fig. 8. This problem has been solved by Hirsh [1] using the same technique for  $Re = 100$ , and by others using different techniques. In this study solutions are obtained for  $Re = 100$  and  $Re = 1000$  on  $21 \times 21$  and  $41 \times 41$  grids respectively. Fig. 9 shows the vorticity and stream function contours for  $Re = 100$ . The contour levels plotted correspond with the values plotted by Hirsh [1]. Qualitatively, the plots appear to be identical.

In Figs. 10-12 the vorticity along the wall, the horizontal velocity  $u$  along the vertical centerline and the vertical velocity  $v$  along the horizontal centerline are compared with a second order central difference CD scheme on  $21 \times 21$  grid and with the results of Ghia et al [16] on  $129 \times 129$  grid. The present results are comparable to the results from the fine grid in [16]. Figs. 13-15 are the same type

of plots for the case  $Re = 1000$  on a  $41 \times 41$  grid. Present results for this case are also in good agreement with results from the fine grid in [16].

## 5.0 CONCLUSIONS

A fourth-order Hermitian compact finite-difference scheme has been successfully applied for solving the two-dimensional, incompressible Navier-Stokes equations in vorticity-stream function form. The steady, laminar flow in the inlet section of a 2-D channel and the flow in a driven square cavity have been chosen as test cases to determine the accuracy of the scheme. An implicit ADI time marching procedure is employed until the steady state solutions are obtained. Results obtained compare favorably with a standard second order central difference and a multi-grid fine-mesh solution.

## ACKNOWLEDGEMENT

The authors acknowledge the support of the Ministry of Science, Technology and Environment, Malaysia, under the IRPA grant No. 09-02-04-0179.

## REFERENCES

1. Hirsh, R., 1975, *Higher Order Accurate Difference Solutions of Fluid Mechanics Problems by a Compact Differencing Technique*, Journal of Computational Physics, vol. 19, pp. 90-109.
2. Adam, Y., 1977, *Highly Accurate Compact Implicit Methods and Boundary Conditions*, Journal of Computational Physics, vol. 24, pp. 10-22.
3. Lele, S. K., 1992, *Compact Finite Difference Schemes with Spectral-Like Resolution*, Journal of Computational Physics, vol. 103, pp.16-42.
4. Deng, X. and Maekawa, H., 1997, *Compact High-Order Accurate Nonlinear Schemes*, Journal of Computational Physics, vol. 130, pp.77-91.
5. Visbal, M. R. and Gaitonde, D. V., 1999, *High-Order-Accurate Methods for Complex Unsteady Subsonic Flows*, AIAA Journal, vol. 10, pp. 358-366.
6. Ekaterinaris, J. A., 2000, *Implicit High-Order-Accurate-in-Space Algorithms for the Navier-Stokes Equations*, AIAA Journal, vol. 38.
7. Rubin, S. G. and Khosla, P. K., 1977, *Polynomial Interpolation Methods for Viscous Flow Calculations*, Journal of Computational Physics, vol.24, pp. 217-244.
8. Luchini, P., 1991, *Higher-Order Difference Approximations of the Navier-Stokes Equations*, International Journal for Numerical Methods in Fluids, vol. 12, pp 491-506.

9. MacKinnon, R. J. and Carey, G. F., 1988, *Analysis of Material Interface Discontinuities and Superconvergent Fluxes in Finite Difference Theory*, *Journal of Computational Physics*, vol. 75, pp.151-167.
10. Abarbanel, S. and Kumar, A., 1988, *Compact High-Order Schemes for the Euler Equations*, *Journal of Scientific Computing*, vol. 3, pp. 275-288.
11. Lax, P. D. and Wendroff, B., 1964, *Difference Schemes for Hyperbolic Equations with High-Order of Accuracy*, *Communications in Pure and Applied Mathematics*, vol. 17, pp. 381-398.
12. Spatz, W. F., 1995, *High-Order Compact Finite Difference Schemes for Computational Mechanics*, Ph. D. Dissertation, The University of Texas at Austin.
13. Asrar, W., Basri, S. and Arora, P. R., 2000, *High Order Compact Solution of the Transient Diffusion Equation*, *Journal – Institution of Engineers, Malaysia*, vol. 61, pp. 41-46.
14. Asrar, W., June, L.W., and Fakir, M.M., 2001, *Fourth-Order Accurate Finite Difference Solution of The Transient Heat Transfer Equation*, *Jurnal Mekanikal*, No. 11, pp 17-26.
15. Mawlood, M. K., Asrar, W. and Basri, S., 2001, *High-Order Compact Finite Difference Solution of Two-Dimensional Problems*, Report No. UPM/FK/KAA/CFD/1/2001.
16. Ghia, U., Ghia, K. N. and Shin, C. T., 1982, *High-Re Solutions for Incompressible Flow Using the Navier-Stokes Equations and a Multigrid Method*, *Journal of Computational Physics*, vol.48, pp. 387-411.

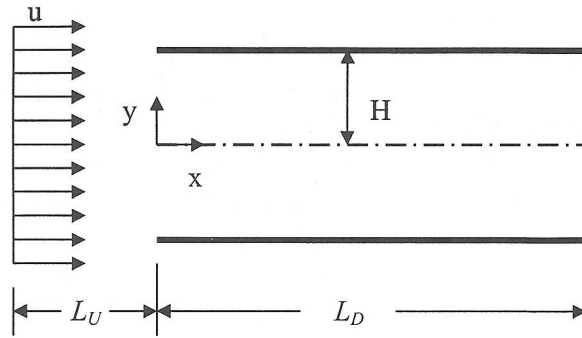


Figure 1 The 2D channel flow geometry

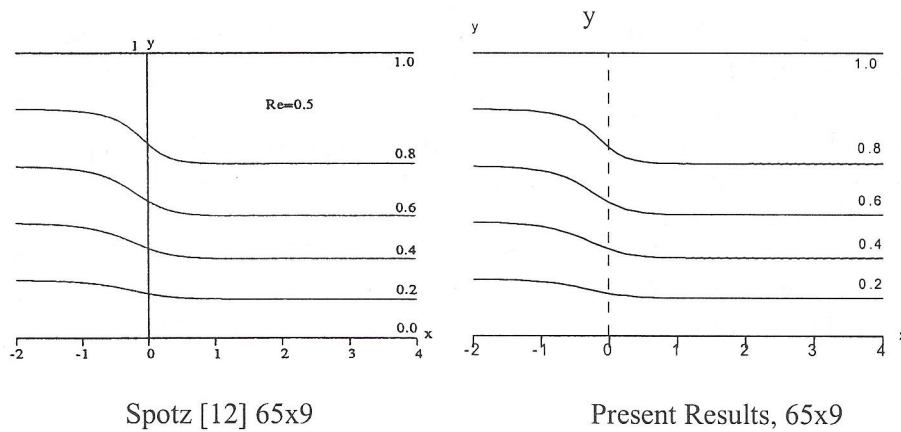


Figure 2 Stream function contours for the 2D channel problem,  $Re = 0.5$

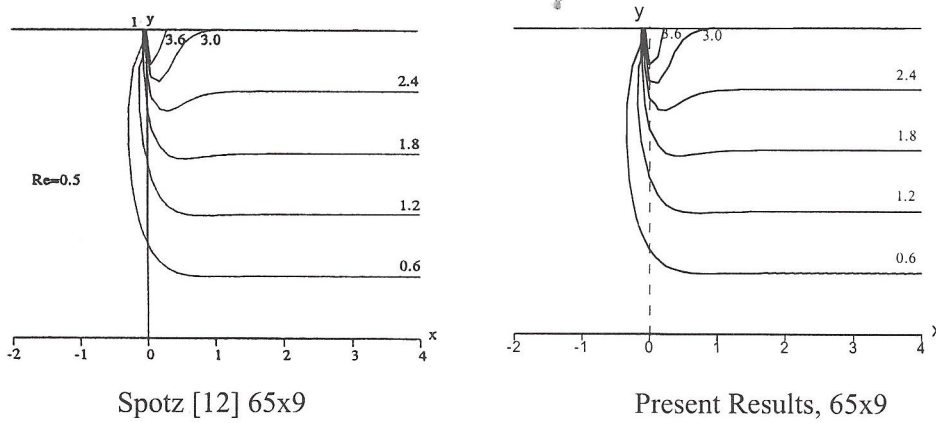


Figure 3 Vorticity contours for the 2D channel problem,  $Re = 0.5$



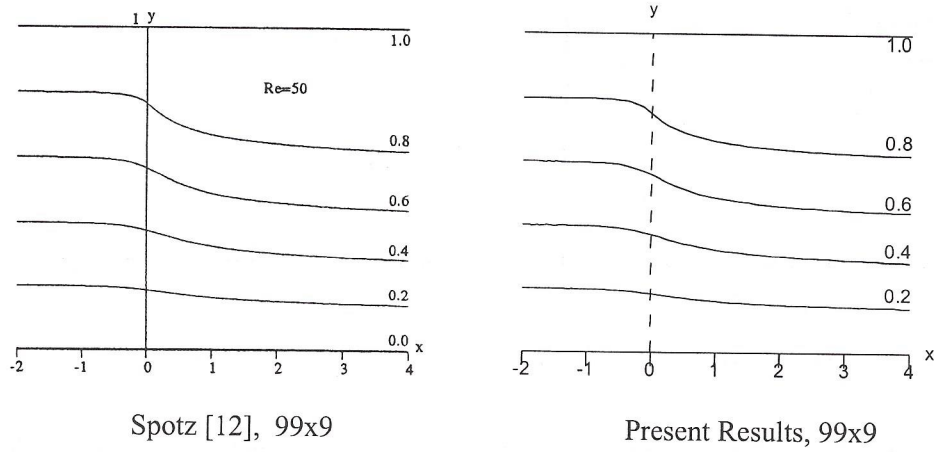


Figure 4 Stream function contours for 2D channel problem,  $Re = 50$

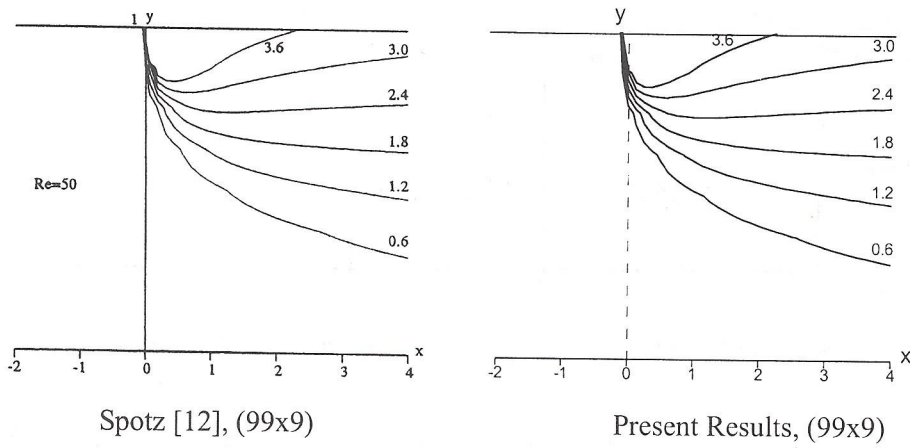


Figure 5 Vorticity contours for the 2D channel problem,  $Re = 50$

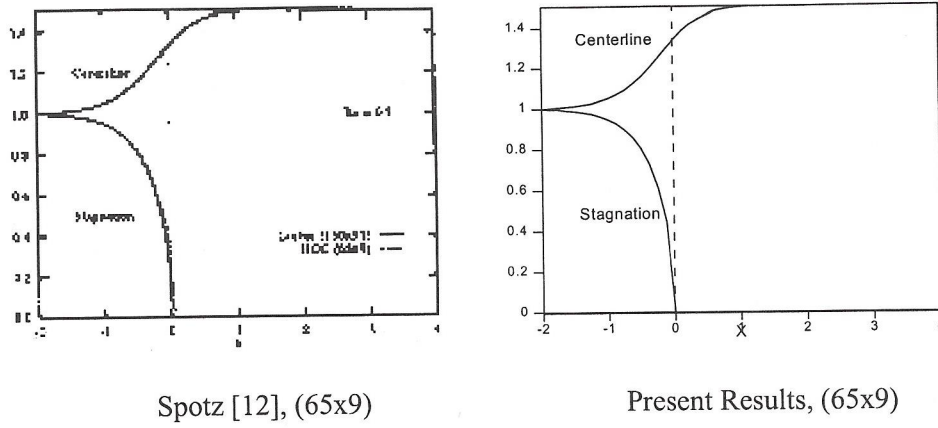


Figure 6 Stagnation and centerline velocity plots for 2D channel problem,  $Re = 0.5$

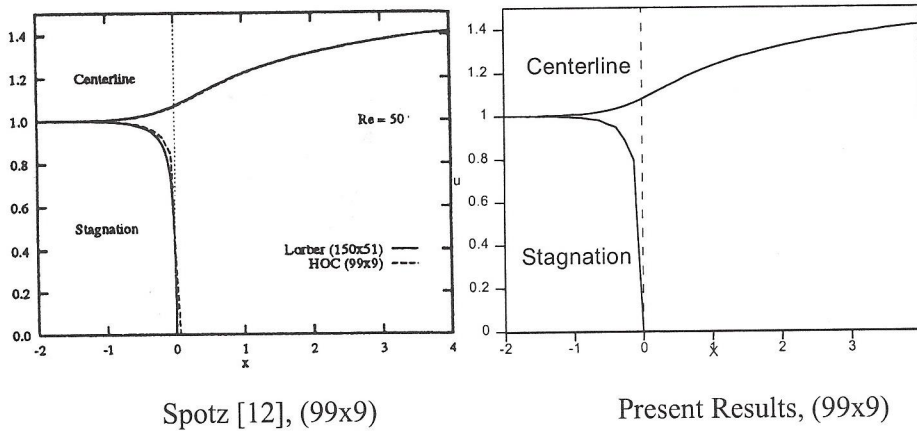


Figure 7 Stagnation and centerline velocity plots for 2D channel problem,  $Re = 50$

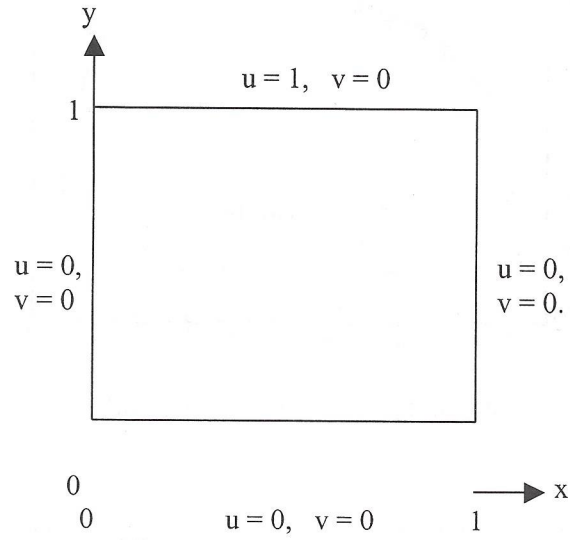


Figure 8 Schematic of driven cavity

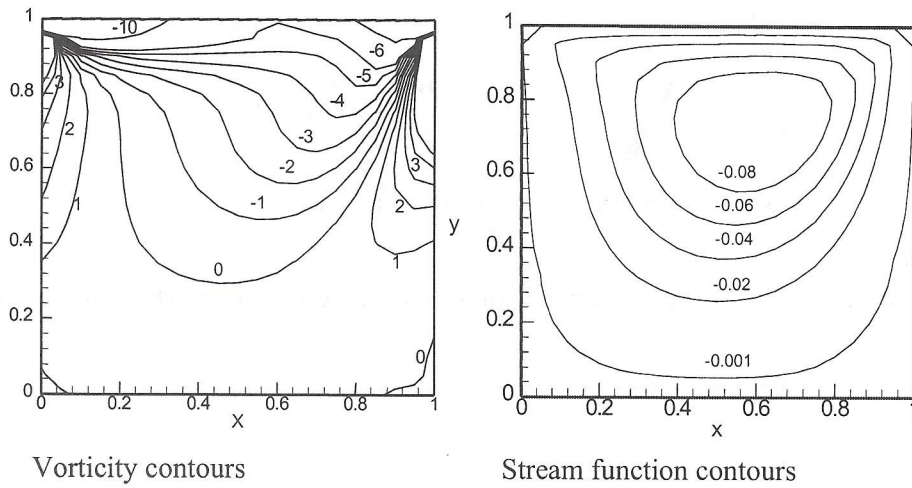


Figure 9 Vorticity and stream function contours for the driven cavity problem,  $Re = 100$

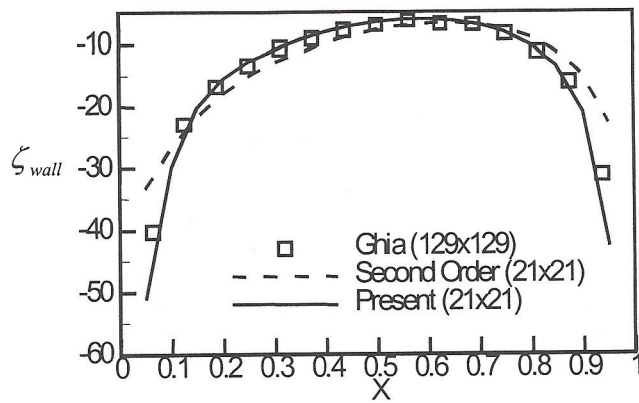


Figure 10 Vorticity along the moving wall , Re = 100

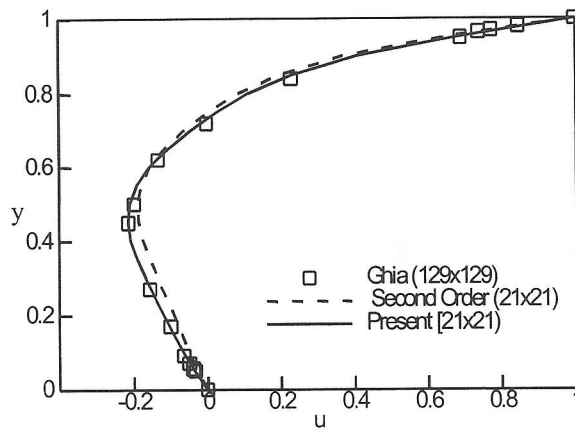


Figure 11 Horizontal velocity component along the vertical centerline, Re = 100

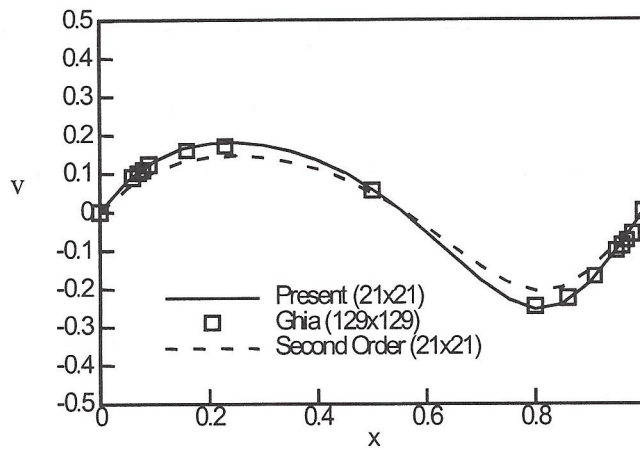


Figure 12 Vertical velocity component along the horizontal centerline, Re = 100

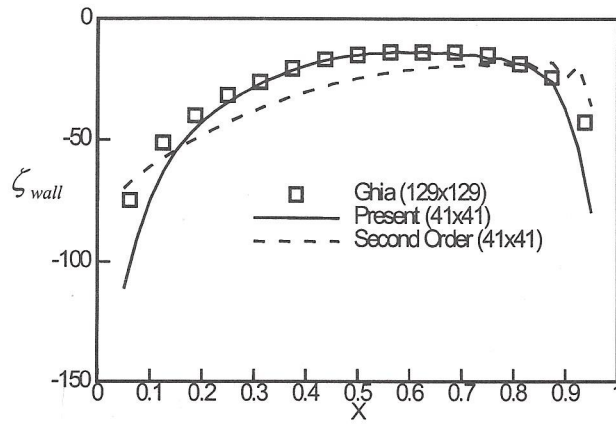


Figure 13 Vorticity along the moving wall, Re = 1000

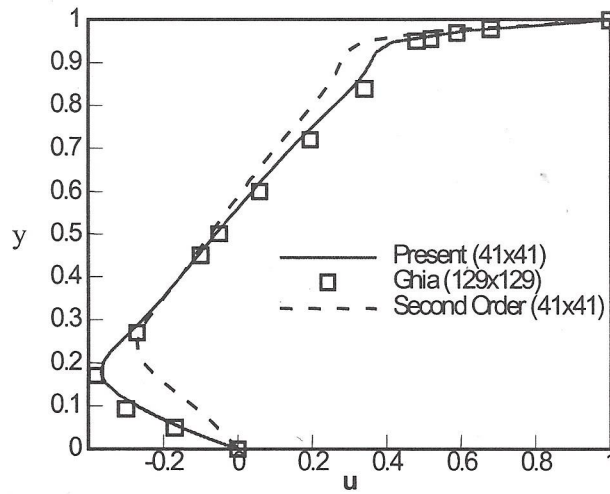


Figure 14 Horizontal velocity component along the vertical centerline, Re = 1000

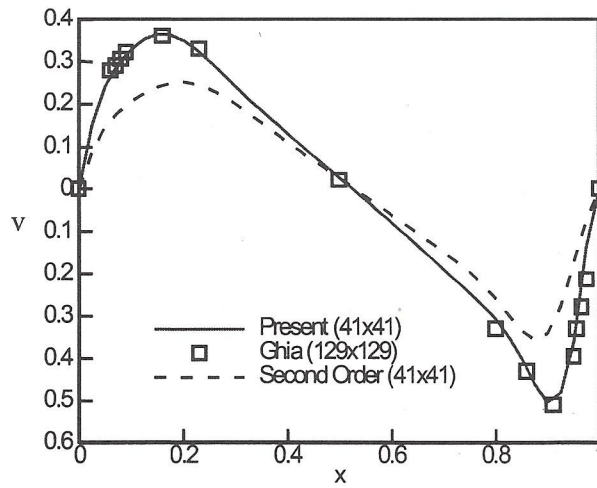


Figure 15 Vertical velocity component along the horizontal centerline, Re = 1000

